Globular Cluster Luminosity Functions and the Hubble Constant from WFPC2 Imaging: The Giant Elliptical NGC 4365[1]

Duncan A. Forbes

Lick Observatory, University of California, Santa Cruz, CA 95064

Electronic mail: forbes@lick.ucsc.edu

Received ____________________; accepted ____________________

[1]Based on observations with the NASA/ESA *Hubble Space Telescope*, obtained at the Space Telescope Science Institute, which is operated by AURA, Inc., under NASA contract NAS 5–26555

ABSTRACT

The turnover, or peak, magnitude in a galaxy's globular cluster luminosity function (GCLF) may provide a standard candle for an independent distance estimator. Here we examine the GCLF of the giant elliptical NGC 4365 using photometry of $\sim$ 350 globular clusters from the *Hubble Space Telescope's* Wide Field and Planetary Camera 2 (WFPC2). The WFPC2 data have several advantages over equivalent ground–based imaging. The membership of NGC 4365 in the Virgo cluster has been the subject of recent debate. We have fit a Gaussian and t_5 profile to the luminosity function and find that it can be well represented by a turnover magnitude of m_V^0 = 24.2 $\pm$ 0.3 and a dispersion σ = 1.28 $\pm$ 0.15. After applying a small metallicity correction to the 'universal' globular cluster turnover magnitude, we derive a distance modulus of (m – M) = 31.6 $\pm$ 0.3 which is in reasonable agreement with that from surface brightness fluctuation measurements. This result places NGC 4365 about 6 Mpc beyond the Virgo cluster core. For a V_{CMB} = 1592$\pm$ 24 km s^{-1} the Hubble constant is $H_\circ = 72^{+10}_{-12}$ km s^{-1} Mpc^{-1}. We also describe our method for estimating a local specific frequency for the GC system within the central 5 h^{-1} kpc which has fewer uncertain corrections than a total estimate. The resulting value of 6.4 $\pm$ 1.5 indicates that NGC 4365 has a GC richness similar to other early type galaxies.

1. Introduction

The measurement and interpretation of extragalactic distances are problematic and often the subject of dispute. In a review of techniques for measuring distances, Jacoby *et al.* (1992) describe five methods that can be applied to elliptical galaxies, namely planetary nebula luminosity functions (PNLF), novae, surface brightness fluctuations (SBF), the $D_n - \sigma$ relation and globular cluster luminosity functions (GCLF). In the case of the GCLF method, the 'standard candle' is the magnitude of the turnover, or peak, in the luminosity function. Although there is no generally accepted theoretical basis, all well–studied globular cluster (GC) systems reveal a similar GCLF shape (often approximated by a Gaussian) with a turnover magnitude of $M_V^0 \sim -7.5$. Measurement of distances, and hence the Hubble constant $H_\circ$, with this method, rely on the assumption that the turnover is the same for all galaxies. Recently there have been claims that the turnover magnitude is not quite constant, but has a slight dependency ($\sim$ 0.2 mag) on GC metallicity (Ashman, Conti & Zepf 1995) or the dispersion in the GCLF, which in turn may reflect a galaxy Hubble type dependence (Secker & Harris 1993).

There have been two recent developments of direct relevance to GCLF–determined distances. The first is due to the much improved Strehl ratio (image concentration) of the second Wide Field and Planetary Camera (WFPC2) on the *Hubble Space Telescope*. Now even relatively short exposures of ellipticals with WFPC2 can contain hundreds of GCs, several magnitudes fainter than typical ground–based observations. To date, published distance measurements based on WFPC2 studies of the GCLF have been carried out by Baum *et al.* (1996) on NGC 4881 in Coma and by Whitmore *et al.* (1995) on M87 in Virgo. These studies quote values of $H_\circ$ = 67 and 78 km s^{-1} Mpc^{-1} respectively. The second development is a new calibration of Galactic GC distances based on revised RR Lyrae luminosities by Sandage & Tammann (1995) which gives an absolute turnover magnitude of M_V^0 = –7.60 ± 0.11 for our Galaxy. Combined with the halo GCs in M31, they derive M_V^0 = –7.62 with an internal error of ± 0.08 and external error of ± 0.2 mags.

Sandage & Tammann (1995) went on to re–analyze ground–based GCLFs for five Virgo ellipticals. Although they derive a distance modulus similar to that of Secker & Harris (1993) for Virgo, they disagree on a couple of issues. In particular, Sandage & Tammann question the dependence of M_V^0 on the GCLF dispersion claiming that it is in part an artifact of the fitting procedure. They also disagree on the cluster membership of one galaxy – NGC 4365. Secker & Harris claim that it lies slightly more distant than the Virgo cluster in the W cloud, as supported by the surface brightness fluctuation (SBF) measurements of Tonry, Ajhar & Luppino (1990). Sandage & Tammann (1995), on the other hand, suggest that the high metallicity of NGC 4365 makes the SBF method unreliable. Both of these GCLF studies used data from Harris *et al.* (1991) and they both derived a m_V^0 for NGC 4365 to be about 0.8 mags fainter than typical Virgo ellipticals. However the uncertainty on this value is much larger than for the other Virgo ellipticals in the Harris *et al.* (1991) data set.

A WFPC2 study of the GCLF for NGC 4365 would have several advantages to help resolve the issue of Virgo membership and further test the hypothesis of a universal GCLF. As well as providing an independent data set, the benefits include very low background contamination, no serious blending effects, accurate photometry and the ability to probe to faint magnitude levels. The galaxy itself is also of interest as it has a relatively high Mg_2 index (Davies *et al.* 1987), contains a kinematically–distinct core which is detectable as a disk–like structure in both the kinematics (Surma 1992) and photometry (Forbes 1994), and has a notably blue nucleus (Carollo *et al.* 1996).

Forbes *et al.* (1996) presented WFPC2 data on the GCs in 14 ellipticals with kinematically–distinct cores (KDC). In that paper we discussed the colors, radial and azimuthal distribution of the GCs. Analysis of the GCLFs were not attempted. Here we analyze the GCLF of NGC 4365, the richest GC system in the Forbes *et al.* study. After determining a completeness function and quantifying the photometric errors, we use the maximum likelihood method of Secker & Harris (1993) to determine the turnover magnitude and dispersion of the GCLF. Within the assumptions of the GCLF–distance method, this leads to an independent estimate of the Hubble constant $H_{\circ}$.

2. Observations and Data Reduction

Details of the WFPC2 data for the NGC 4365 GCs are presented, along with 13 other KDC ellipticals, in Forbes *et al.* (1996). Briefly, two 500s F555W images were combined, as were two 230s F814W images. Using DAOPHOT (Stetson 1987), GCs were detected in the F555W image only, their magnitudes measured and then the corresponding F814W magnitudes were determined. The magnitudes have been converted into the standard Johnson–Cousins V, I system and corrected for Galactic extinction. We chose a fairly conservative detection criteria based on flux threshold, shape, sharpness and size. Additionally, we checked the positions of GCs against a list of known hot pixels. After these criteria have been applied, we are confident that the contamination from cosmic rays, hot pixels, foreground stars and background galaxies is small (less than a few percent) in our object list. Forbes *et al.* (1996) made one additional cut, namely $\pm 3\sigma$ about the mean color of V–I = 1.10. Here we have chosen to use only the V band data (which is of higher signal-to-noise than the I band data) and not apply any selection based on color.

The detection flux threshold in the PC image was set lower than the WFC images, to compensate for the different point source sensitivity (i.e. $\sim$0.3 mags; Burrows *et al.* 1993). In Figure 1 we show the fraction of actual GCs detected as a function of GC magnitude, normalized at V = 25. This figure shows that the resulting detection fractions are similar between all four CCDs.

3. Modeling

3.1. Completeness Function

Forbes *et al.* (1996) carried out simulations to quantify the ability of DAOPHOT to detect GCs as a function of magnitude. A typical WFC image was chosen for the simulation. The resulting completeness function showed that all GCs brighter than V $\sim$ 24 were detected, and the completeness dropped off rapidly to V $\sim$ 25. As it is crucial for GCLF studies to have a well–determined completeness function we have decided to redo the simulation using the WF3 image of NGC 4365 to ensure that we have the same photon and read noise characteristics as the data. We note that there is no evidence for a significant variation between CCDs. We have simulated GCs using the *addstar* task and then used DAOPHOT with the same detection criteria as for the actual GCs. In particular, we have excluded all objects with FWHM sizes greater than three pixels. For these simulations $\leq$ 1% of the objects are excluded by this criterion. As with the real data, we have not attempted to reject any objects based on color.

The completeness function resulting from simulations of 900 artifical GCs is shown in Figure 2a. This function is similar to that given in Forbes *et al.* (1996). We derive a 50% completeness level at V = 24.7. For the subsequent analysis the completeness function is set to zero for magnitudes fainter than this to avoid incompleteness corrections larger than a factor of two.

3.2. Photometric Errors

In addition to the completeness function we need to quantify the photometric, or measurement, error from DAOPHOT. Photometric errors can cause a shift of the GCLF peak to brighter magnitudes, as the fainter GCs, with relatively large errors, move into brighter magnitude bins. This 'bin jumping' effect is described in detail by Secker & Harris (1993) and taken into account in their maximum likelihood technique. Here we have fit the DAOPHOT determined errors with an exponential of the form:

$$\text{p.e.} = \exp\left[a\,(V - b)\right]$$

The photometric error and the fit as a function of V magnitude are shown in Figure 2b. Reassuringly these errors are similar to those found by comparing the input and measured magnitudes of the simulated GCs. A typical photometric error is $\pm$ 0.1 mag at V = 24.

3.3. Background Contamination

One of the advantages of using WFPC2 data for GCLF studies is the ability to exclude most foreground stars and background galaxies based on angular size. This means that the contamination from such sources is very low. Nevertheless we estimated the background contamination on a similar exposure time WFPC2 image from the Medium Deep Survey (Forbes *et al.* 1994). Again we used DAOPHOT to detect objects with the same detection parameters as before, including the same size criteria as for the GCs. No color selection was used. We estimate a background contamination of seven objects, brighter than V = 24.7, in the WFPC2 field-of-view.

3.4. Maximum Likelihood Technique

In this study we use the maximum likelihood technique of Secker & Harris (1993) to accurately determine the GCLF peak magnitude and dispersion. Their technique is designed to take proper account of detection incompleteness at faint magnitudes, photometric error and background contamination. It calculates the convolution product of the photometric error and the intrinsic GCLF, weighted by the completeness function. This is then compared to the raw data set, and after allowing for the background contamination, gives the most likely parameters of the intrinsic GCLF. As well as the commonly used Gaussian profile, we fit a t_5 distribution which is less susceptible to variations at the extremes of the luminosity function. The t_5 distribution function has the form:

$$\mathrm{N}(m) = A(1 + (m - m^0)^2/5\sigma_t^2)^{-3}$$

Where A is a scaling constant and σ_t is the GCLF dispersion, which is related to the dispersion of a Gaussian by $\sigma_t \sim 0.78\sigma_G$ (see Secker 1992 for details of the t_5 function).

4. Results and Discussion

After applying the maximum likelihood code to our sample of 346 GCs with V $<$ 24.7, we find the best estimate and uncertainty for a Gaussian profile fit to the GCLF to be m_V^0 = 24.17 (+0.3,–0.3), σ = 1.36 (+0.14,–0.15). For a t_5 profile fit, we find m_V^0 = 24.00 (+0.3,–0.2), σ = 1.17 (+0.15,–0.13). These errors represent the collapsed one–dimensional confidence limits for one standard deviation. The probability contours output from the maximum likelihood code for the Gaussian fit, over a range of 0.5–3 standard deviations, are shown in Figure 3. The contours are skewed towards a larger dispersion and fainter magnitudes, giving rise to the asymmetric errors quoted above. A similar effect can be seen in the ground–based data of NGC 4365 by Secker & Harris (1993). Although the quoted errors represent the internal error of the fitting procedure, they dominate over any contribution from photometric errors. As a test, we increased the photometric errors by 20% (which represents the extreme range of photometric errors from DAOPHOT) and refit the data. This gave a turnover magnitude and dispersion different by < 3%. In Figure 4 we show a binned GCLF and our best–fit Gaussian superposed. Note that the fitting procedure does not use binned data but rather treats each data point individually.

Secker & Harris (1993) have shown that the GCLF parameters will be systematically biased towards brighter magnitudes and smaller dispersions if the limiting magnitude is close to or brighter than the true turnover magnitude. Our limiting magnitude has been set at the 50% completeness level, i.e. V = 24.7. Using their figure 6, the true turnover magnitude for a t_5 distribution is $\sim$ 0.1 mag fainter and the dispersion 0.05 mag larger. The results of the two fitting methods, after applying this bias correction to both results, are listed in Table 1. Averaging the results from the two fitting methods, gives $m_V^0 = 24.2 \pm 0.3$ and $\sigma = 1.28 \pm 0.15$, which is a reasonable representation of the turnover and dispersion of our V band data for the GCLF of NGC 4365. We also list the results of Secker & Harris for the B band GCLF. If we assume that the NGC 4365 GCs have B–V $\sim$ 0.9, then their turnover is fainter by $\sim$ 0.2 mags. We find a slightly smaller GCLF dispersion. The quoted errors are similar between the two studies.

An additional small correction may be required if we wish to compare the magnitudes of the NGC 4365 GCs with the 'universal value' (i.e. the mean of the Milky Way and M31 systems from Sandage & Tammann 1995). As mentioned in the introduction, Secker & Harris (1993) and also Fleming *et al.* (1995) suggest that the GCLF turnover depends on Hubble type. Compared to nearby spirals, the more luminous ellipticals have a fainter turnover. On a more quantitative basis, Ashman *et al.* (1995) have suggested that GC metallicity is the second parameter, with more metal rich GCs having a fainter turnover.

These ideas can be connected via the GC metallicity–galaxy luminosity relation (e.g. Brodie & Huchra 1991, Forbes *et al.* 1996) in which more luminous galaxies (e.g. giant ellipticals) have relatively metal rich GC systems. Ashman *et al.* showed that if these metallicity–based corrections were applied to the turnover GC absolute magnitude, then the systematic offset between GCLF distance estimates and other methods (see Jacoby *et al.* 1992) could be largely eliminated.

In the absence of spectroscopic measures, the mean metallicity of the GC system in NGC 4365 can be estimated crudely from the V–I colors of the GCs. Using the GC sample described in section 2, we calculate a mean metallicity, assuming [Fe/H] = 5.051 (V–I) – 6.096 (Couture *et al.* 1990), of [Fe/H] = –0.6. The mean metallicity of the Milky Way and M31 GCs, using the same relative weighting as Sandage & Tammann (1995) is [Fe/H] = –1.4. Applying Table 3 of Ashman *et al.* gives ΔM_B^0 = 0.37 and ΔM_V^0 = 0.23 for a metallicity difference of 0.8 dex. (A metallicity difference of 0.7–0.9 dex would correspond to roughly ΔM_B^0 = 0.32–0.45 and ΔM_V^0 = 0.18–26.) These corrections make the combined Milky Way and M31 peaks of M_B^0 = –6.93 ± 0.08 and M_V^0 = –7.62 ± 0.08 (Sandage & Tammann 1995) fainter by 0.37 and 0.22 respectively. Combining these M^0 values with m^0 from Table 1 gives the distance modulus for both the Gaussian and t_5 fits. The fits and the averages (with errors added in quadrature and divided by $\sqrt{N}$) are listed in Table 2. From our data the t_5 and Gaussian fits give $(m - M)$ = 31.6 ± 0.3.

An independent estimate of the distance modulus comes from surface brightness fluctuation (SBF) measurements (Tonry, Ajhar & Luppino 1990). Ajhar *et al.* (1994) quote an SBF distance modulus of 31.74 ± 0.16 for NGC 4365, based on the latest calibration of Tonry (1991), which is given in Table 2. The two GCLF distance determinations are in good agreement with that from the SBF method.

We also list in Table 2, recent determinations for the distance modulus to the Virgo galaxies NGC 4472 (M86), NGC 4486 (M87) and NGC 4649 using the GCLF method. Again the distance modulus is calculated using either $M_B^0 = -6.93 \pm 0.08$ or $M_V^0 = -7.62 \pm 0.08$ and a metallicity correction from Ashman *et al.* (1995), with GC mean metallicities as compiled by Perelmuter (1995). These three galaxies give a GCLF distance modulus to Virgo of about $(m - M) = 31.25 \pm 0.15$ (internal error only), which can be compared to the weighted mean from 6 different methods (i.e. novae, SN Ia, Tully–Fisher, PNLF, SBF and D_n–σ) of $(m - M) = 30.97 \pm 0.18$.

To summarize, the GCLF method indicates a similar distance to the Virgo cluster as other distance methods, and the GCLF and SBF distances to NGC 4365 are in good agreement. However, the distance modulus for NGC 4365 is 0.5–0.75 magnitudes fainter than that for the Virgo core. This would suggest it is 25–40% more distant than the Virgo core. Using a representative GCLF distance modulus of $(m - M) = 31.74 \pm 0.3$ gives a distance of 22.28 (+3.31, –2.87) Mpc.

It is of course interesting to take the distance calculation one step further and estimate the Hubble constant from this one galaxy. The velocity of NGC 4365 with respect to the cosmic microwave background is $V_{CMB} = 1592$ km s^{-1} (Faber *et al.* 1989). We assume an error on this value to be the fractional error from the radial velocity measurement by Huchra *et al.* (1983), i.e. $\pm$ 24 km s^{-1}. Dividing this velocity by 22.28 Mpc gives a Hubble constant of 72 (+10, –12) km s^{-1} Mpc^{-1}. The velocity from the D_n–σ relation is similar, i.e. 1509 $\pm$ 250 km s^{-1} after making a $\sim$3% correction for the Malmquist bias (Faber *et al.* 1989). This would give a Hubble constant of 68 (+21, –20) km s^{-1} Mpc^{-1}.

Another measure of interest is the specific frequency (S) of the GC system, which gives an indication of the relative richness of the GC system, and is defined by:

$$S = N 10^{0.4(M_V + 15)}$$

Where N is usually the total number of GCs and M_V the total galaxy magnitude. Estimates of S for galaxies beyond the local group require two, sometimes large and uncertain, corrections for the number of faint GCs that weren't detected and the limited areal coverage. Starting with the first correction, by integrating under our profile fit to the GCLF we make can make a fairly accurate estimate of the total number of GCs within the WFPC2 field-of-view. The t_5 and Gaussian fits give a total of 522 and 554 GCs respectively, over all magnitudes. Taking the average of these we get 538 GCs. We find that 84.7% of the NGC 4365 GCs lie within a 180° hemisphere of radius $100''$ (5 h^{-1} kpc). The total number of GCs within a $100''$ radius circle is twice this amount or 911 (with an estimated error of ±12%). Knowing the integrated galaxy absolute magnitude within this radius will give us a 'local' S value. From the surface photometry of Goudfrooij *et al.* (1994), we calculate a magnitude of V = 11.36 ± 0.1, and using $(m - M)$ = 31.74 ± 0.3, gives a localized specific frequency of S = 6.4 ± 2.7. The second correction, calculating the total number in the GC system, is much more uncertain. This can be estimated by integrating the density profile found by Forbes *et al.* (1996) out to large radii, with the boundary condition that at r = $100''$, the number of GCs is 911. This gives a total for the GC system of N = 2511 ± 1000, which can be compared to N = 3500 ± 1200, from ground–based imaging, estimated by Harris (1991). Using a total V = 9.65 ± 0.1 (Faber *et al.* 1989) and the same distance modulus as above, gives M_V = –22.09 ± 0.32 and S = 3.7 ± 2.4. Our estimated S values, 6.4 and 3.7, are similar to the average value of 5.1 for 34 E+S0 galaxies (van den Bergh 1995). Harris (1991) quoted 7.7 ± 2.7 for NGC 4365. Part of the difference is due to our lower number of GCs and also because Harris, assumed that NGC 4365 was in Virgo with a distance modulus of 31.3. For N = 3500 ± 1200 and our a distance modulus of 31.74 ± 0.3, S = 5.1 ± 3.3.

5. Conclusions

We have used the *HST* WFPC2 data of Forbes *et al.* (1996) to examine the luminosity function of ∼350 globular clusters in the central regions of the giant (M_V = –22.1) elliptical NGC 4365. In particular, we fit the globular cluster luminosity function (GCLF) by both a Gaussian and t_5 distribution, using the maximum likelihood analysis of Secker & Harris (1993). The GCLF is well fit by a turnover magnitude of $m_V^0 = 24.2 \pm 0.3$ and dispersion $\sigma = 1.28 \pm 0.15$ (the two fitting profiles give similar results). Our results are compared to previous work on the GCLF of NGC 4365 and other Virgo ellipticals. Using the most recent determination of the Milky Way and M31 galaxy's GCLF turnover magnitude of Sandage & Tammann (1995), and a metallicity correction based on the precepts of Ashman *et al.* (1995), we derive a distance modulus of 31.6 ± 0.3. This is in reasonable agreement with $(m - M) = 31.74 \pm 0.16$ derived from surface brightness fluctuation measurements of NGC 4365 and provides further support to the hypothesis that the absolute turnover magnitude of GCLFs is approximately constant or 'universal' for all galaxies. Our distance modulus also supports the previous findings from ground–based data that the GCLF turnover is ∼0.7 magnitudes fainter, or ∼6 Mpc more distant, than that of ellipticals in the Virgo cluster core. As such NGC 4365 may lie in the W$'$ group of the SW extension of the Virgo cluster or in the background W cloud (Binggeli, Tammann, & Sandage 1987).

Adopting a velocity, with respect to the cosmic microwave background, for NGC 4365 of V_{CMB} = 1592 ± 24 km s^{-1} gives a Hubble constant of $H_\circ$ = 72 (+10, –12) km s^{-1} Mpc^{-1} (internal errors only). This value lies between recent determinations of $H_\circ$ from the GCLF of NGC 4881 and M87 using WFPC2. After correcting for undetected objects, we have estimated the total number of globular clusters in a 5 h^{-1} kpc radius circle about the galaxy center to be 911. Using the integrated galaxy light within this region, we derive a 'local' specific frequency of S = 6.4 ± 1.5. This measure has the advantage of requiring fewer uncertain corrections than a total estimate. For a distance modulus of 31.74, the ground–based total specific frequency becomes 5 ± 2, which is similar to our local S

value and in excellent agreement with the average S value for a large sample of early type galaxies.

Acknowledgments

We are particularly grateful to J. Secker for the use of his maximum likelihood code and useful suggestions. We also thank R. Elson, C. Grillmair and R. Guzmán for helpful discussions. This research was funded by the HST grant AR-05794.01-94A

References

Ajhar, E. A., Blakeslee, J. P., & Tonry, J. L. 1994, AJ, 108, 2087 (ABT94)

Ashman, K. M., Conti, A., & Zepf, S. E. 1995, AJ, 110, 1164

Baum, W. A., *et al.* 1995, AJ, 110, 2537

Binggeli, B, Tammann, G. A., & Sandage, A. 1987, AJ, 94, 251

Brodie, J. P., & Huchra, J. 1991, ApJ, 379, 157

Burrows, C., *et al.* 1993, Hubble Space Telescope Wide Field and Planetary Camera 2 Instrument Handbook, STScI

Carollo, C. M., Franx, M., Illingworth, G. D., & Forbes, D. A. 1996, ApJ, submitted

Couture, J., Harris, W. E., & Allwright, J. W. B., 1990, ApJS, 73, 671

Davies, R. L., *et al.* 1987, ApJS, 64, 581

Faber, S. M., *et al.* 1989, ApJS, 69, 763

Forbes, D. A. 1994, AJ, 107, 2017

Forbes, D. A., Elson, R. A. W., Phillips, A. C., Illingworth, G. D. & Koo, D. C. 1994, ApJ, 437, L17

Forbes, D. A., Franx, M., Illingworth, G. D., & Carollo, C. M. 1996, ApJ, in press

Harris, W. E. 1991, ARAA, 29, 543

Harris, W. E., Allwright, J. W. B., Pritchet, C. J., & van den Bergh, S. 1991, ApJS, 276, 491

Huchra, J., Davis, M., Latham, D., & Tonry, J. 1983, ApJS, 52, 89

Jacoby, G. H., *et al.* 1992, PASP, 104, 599 (J92)

Perelmuter, J. L. 1995, ApJ, 454, 762

Sandage, A., & Tammann, G. A. 1995, ApJ, 446, 1

Secker, J. 1992, AJ, 104, 1472

Secker, J., & Harris, W. E. 1993, AJ, 105, 1358 (SH93)

Stetson, P. B., 1987, PASP, 99, 191

Surma, P. 1992, Structure, Dynamics and Chemical Evolution of Elliptical Galaxies, ed. I. J. Danziger, W. W. Zeilinger and K. Kjar, ESO: Garching, p. 669

Tonry, J. L., Ajhar, E. A., & Luppino, G. A. 1990, AJ, 100, 1416

Tonry, J. L. 1991, ApJ, 373, L1

van den Bergh, S. 1995, AJ, 110, 2700

Whitmore, B. C., Sparks, W. B., Lucas, R. A., Macchetto, F. D., & Biretta, J. A. 1995, ApJ, in press (W95)

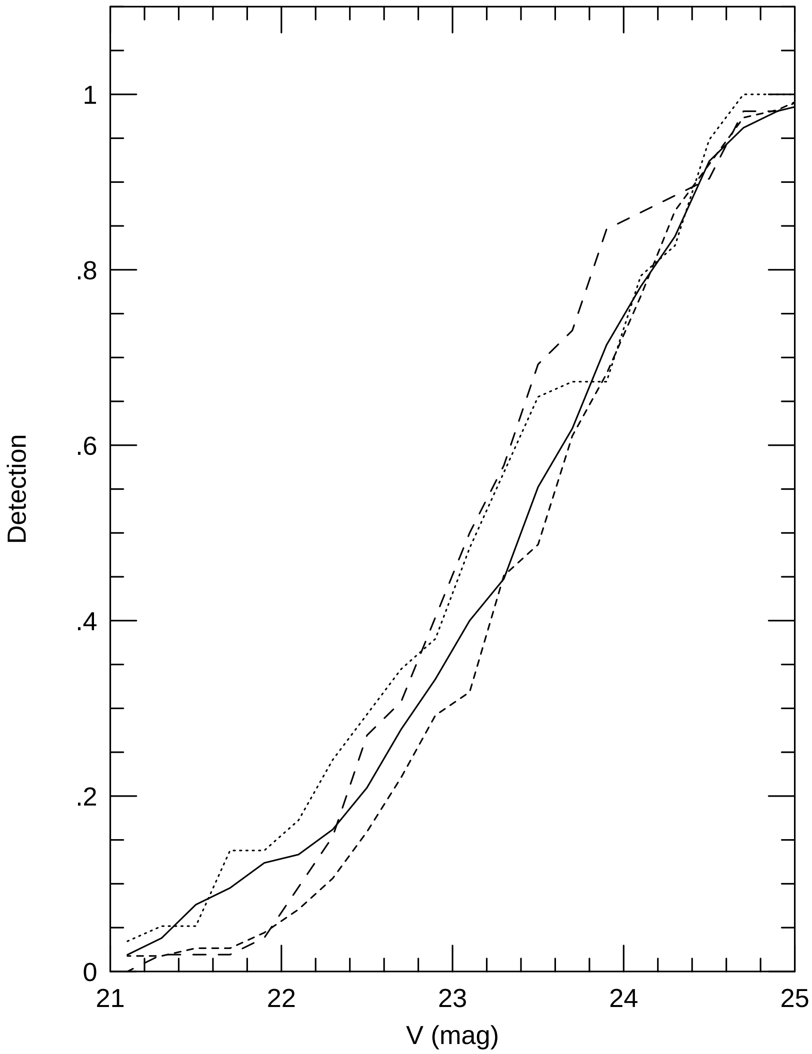

Fig. 1.— Detection of actual globular clusters in each CCD normalized at V = 25. The different CCDs are represented as follows: PC (long dashed), WF2 (short dash), WF3 (dotted) and WF4 (solid). The fraction of actual detected globular clusters in all 4 CCDs is similar to V = 25.

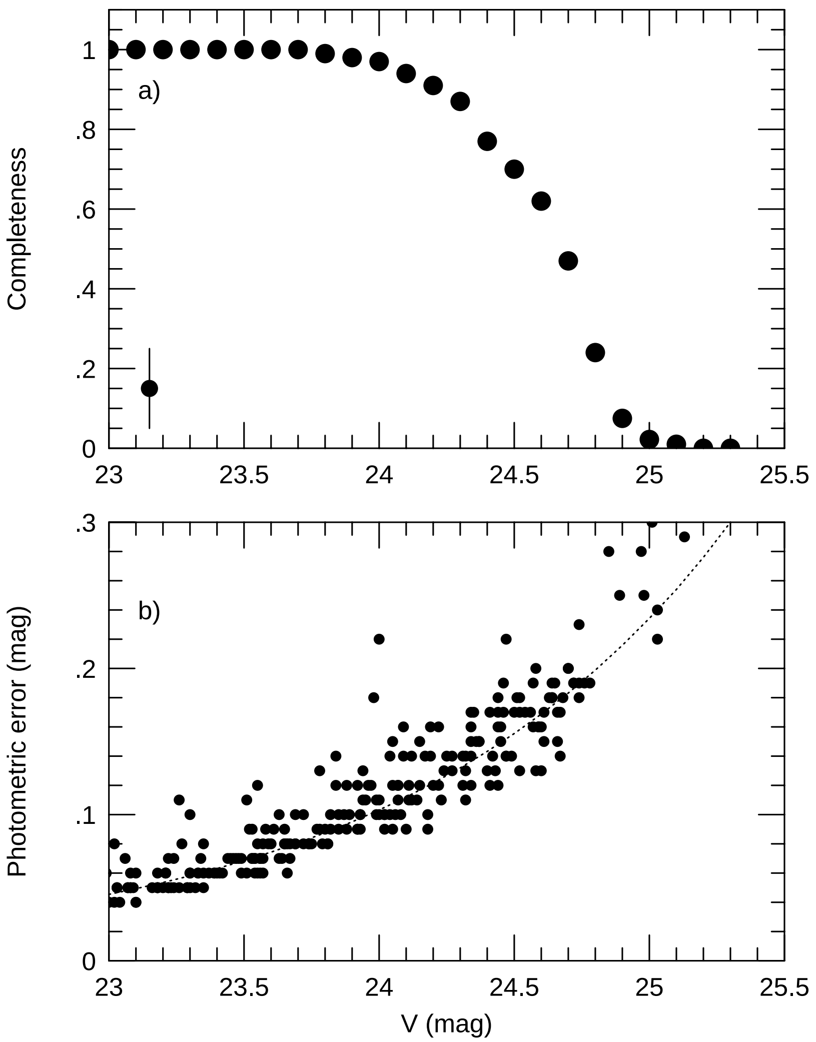

Fig. 2.— Completeness function for GC detection from simulations. Circles show the fraction of simulated GCs detected in 0.1 magnitude bins. A typical error bar is shown in the lower left. **b)** Photometric error as a function of GC V magnitude determined from DAOPHOT. Circles show the data points, and the dashed line an exponential fit to the data of the form p.e. = exp [a (V – b)].

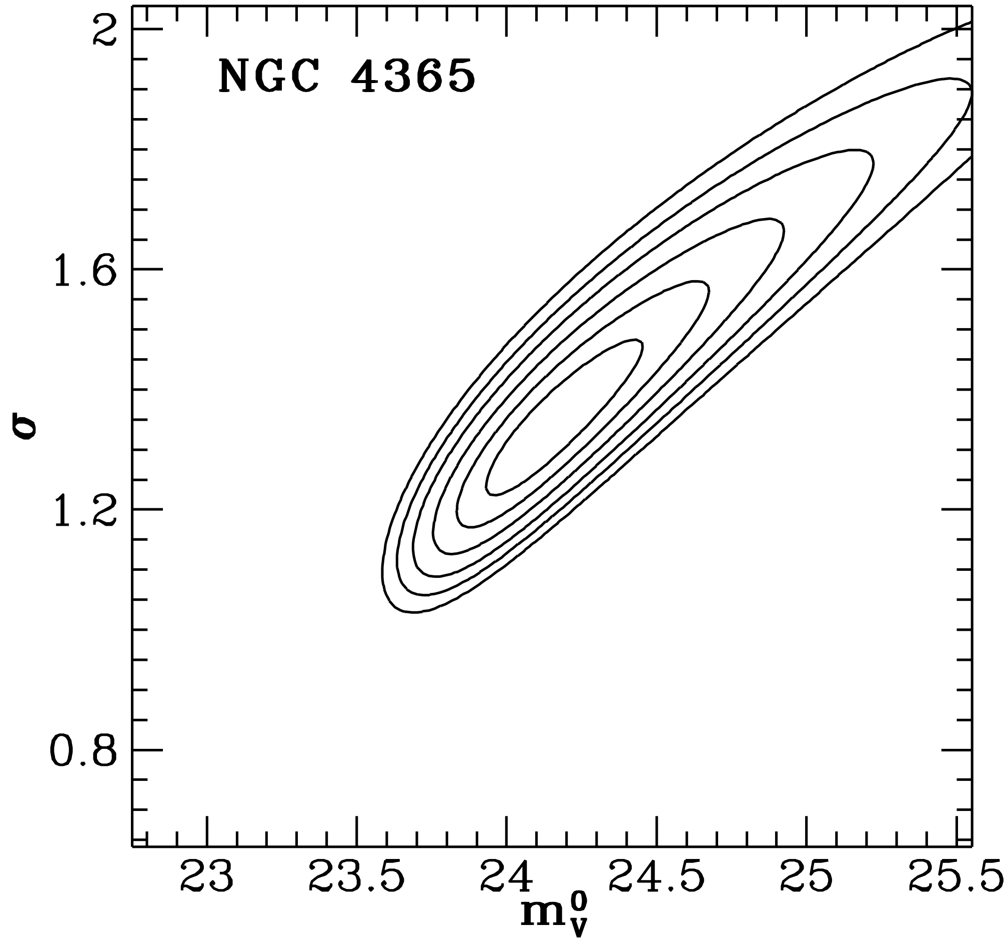

Fig. 3.— Probability contours for the turnover magnitude and dispersion for a Gaussian fit from the maximum likelihood code of Secker & Harris (1993). Contours represent 0.5 to 3 standard deviations probability limits from the best estimate (see Table 1).

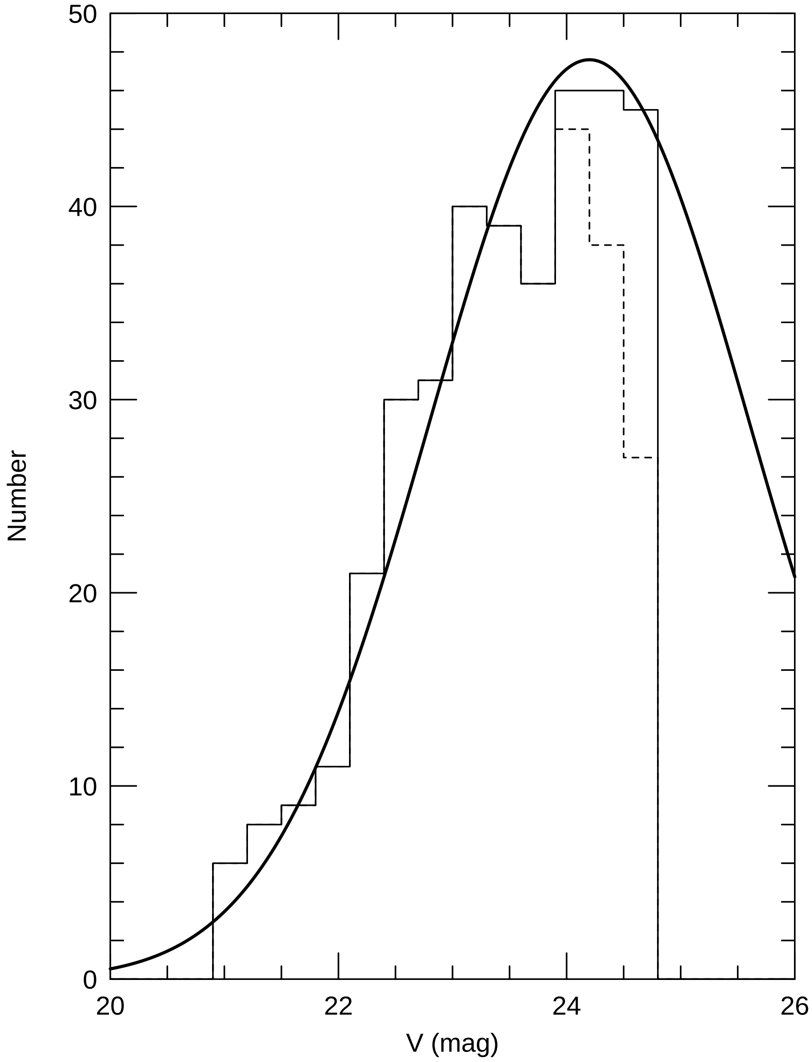

Fig. 4.— Globular cluster luminosity function for NGC 4365. The raw data is shown by a dashed line, and by a thin solid line after completeness correction has been applied. The maximum likelihood best fit Gaussian profile, which includes the effects of photometric error and background contamination, is superposed as a thick solid line. Note that the fitting procedure does not use binned data.

TABLE 1. Globular Cluster Luminosity Function Parameters for NGC 4365

Ref. (1)	m_G^0 (mag) (2)	σ_G (mag) (3)	m_t^0 (mag) (4)	σ_t (mag) (5)
This work (V band)	24.27±0.30	1.41±0.15	24.10±0.25[a]	1.22±0.15
SH93 (B band)	25.31±0.35	1.61±0.17	25.37±0.24	1.52±0.13

Notes to Table 1.

(1) Reference; (2) Apparent magnitude of the GCLF turnover from a Gaussian fit; (3) Dispersion of the GCLF from a Gaussian fit; (4) Apparent magnitude of the GCLF turnover from a t_5 fit; (5) Dispersion of the GCLF from a t_5 fit ([a] actual error is asymmetric, +0.3, −0.2).

TABLE 2

Globular Cluster Luminosity Function Parameters for Virgo Ellipticals

Galaxy (1)	(m−M) (mag) (2)	(Method) (3)	Ref. (4)	(m−M) (mag) (5)	(Method) (6)	Ref. (7)
NGC 4365	31.67 ± 0.31	G GCLF	This work	31.50 ± 0.26	t_5 GCLF	This work
NGC 4365	31.87 ± 0.36	G GCLF	SH93	31.93 ± 0.26	t_5 GCLF	SH93
Average	31.76 ± 0.33	G GCLF	···	31.72 ± 0.26[a]	t_5 GCLF	···
NGC 4365	31.74 ± 0.16	SBF	ABT94	···	···	···
NGC 4472	31.28 ± 0.18	G GCLF	SH93	31.28 ± 0.14	t_5 GCLF	SH93
NGC 4486	31.26 ± 0.11	G GCLF	W95	···	···	···
NGC 4649	31.14 ± 0.17	G GCLF	SH93	31.27 ± 0.14	t_5 GCLF	SH93
Average	31.23 ± 0.16	G GCLF	···	31.28 ± 0.14	t_5 GCLF	···
Virgo core	30.97 ± 0.18	Various	J92	···	···	···

Note.—(1) Galaxy name; (2) Distance modulus assuming either $M_V^0 = -7.62 \pm 0.08$ or $M_B^0 = -6.93 \pm 0.08$ and a metallicity correction (see text for details); (3) Distance modulus method, GCLF fit G = Gaussian, t = t_5 distribution, SBF = surface brightness functions, various = mean of 6 methods excluding GCLF; (4) Reference; (5) Distance modulus ([a] actual error is asymmetric, +0.31, −0.21); (6) Method; (7) Reference.